New SnO₂/MgAl-layered double hydroxide composites as photocatalysts for cationic dyes bleaching

E. Dvininov [a,*], M. Ignat [a], P. Barvinschi [b], M.A. Smithers [c], E. Popovici [a]

[a] Department of Physical and Theoretical Chemistry and Materials Chemistry, "Al. I. Cuza" University, Bd. Carol I, No 11, 700506 Iasi, Romania
[b] Faculty of Physics, West University of Timisoara, Bd. V. Parvan 4, 300223 Timisoara, Romania
[c] MESA⁺ Institute of Nanotechnology, University of Twente, 7500 AE Enschede, Netherlands

ABSTRACT

A new type of nanocomposite containing SnO_2 has been obtained by wet impregnation of dehydrated Mg/Al-hydrotalcite-type compounds with ethanolic solutions of $SnCl_4 \cdot 2H_2O$. Tin chloride hydrolysis was achieved using NaOH or NH_4OH aqueous solutions, at pH around 9, followed by the conversion into corresponding hydroxides through calcinations. The powder X-ray diffraction (PXRD) and UV–Vis diffuse reflectance (UV-DR) methods confirmed the structure of as-synthesized solids. The chemical composition and morphology of the synthesized materials were investigated by energy dispersive X-ray analysis (EDX), scanning electron microscopy (SEM) and transmission electron microscopy (TEM). The as-synthesized materials were used for photocatalytic studies showing a good activity for methylene blue decolourization, which varies with SnO_2 content and used as a hydrolysing agent. The proposed mechanism is based on the shifting of flat band potential of SnO_2 due to the interaction with Mg/Al-LDH, this being energetically favourable to the formation of hydroxyl radicals responsible for methylene blue degradation.

1. Introduction

The presence of organic pollutants (phenols, VOCs, pesticides, dyes, etc.) is of great concern nowadays, the contamination of rivers and ground water acting as stimulus for numerous investigations focused on the effective pollution abatement methods [1]. The currently used approaches to remove the organic pollutants from the waste waters are based on the adsorption or chemical oxidation processes. However, these processes have major drawbacks: the adsorption does not lead to pollutant degradation, while the chemical oxidation, in homogeneous phase, is not economically favourable, except the high concentrated pollutants [2].

Layered materials, such as montmorillonite and hydrotalcite-like compounds, have attracted much attention for waste water remediation and, moreover, their applicability to generate photocatalytic active materials is of major importance due to environmental friendliness [3,4].

Layered double hydroxide (LDH) is the generic name of the materials having general formula: $[M(II)_{(1-x)}M(III)x(OH)_2]^{x+}[(A^{n-})_{x/n} \cdot mH_2O]^{x-}$, where M(II) and M(III) are metal cations and A is an anion. The structure consists of brucite-like layers constituted of edge sharing $M(OH)_6$ octahedra. Partial substitution of the diva-lent cation by a trivalent cation will generate the positive charging of the layers, which is balanced by the presence of the anions in the interlayer spaces. The distance between the layers is a function of both the nature of interlayer species and their interaction with the layers [5].

A large variety of metallic ions, as divalent or trivalent cations: $M^{2+} = Mg^{2+}$, Zn^{2+}, Co^{2+}, Cu^{2+}, Mn^{2+}; $M^{3+} = Al^{3+}$, Fe^{3+}, Cr^{3+}, V^{3+}, Ga^{3+}, Ti^{3+}, were incorporated in octahedral layers [5]. Some hydrotalcite-like compounds with monovalent and tetravalent cations: Li–Al(III), Co–Ti(IV) or Zn–Ti(IV) have been also reported [6,7]. Velu et al. [8,9] have reported partial isomorphous substitution of Al^{3+} with Sn^{4+}, in order to obtain a new Mg–Al–Sn ternary LDH. Using coprecipitation method, Intissar et al. [10,11] have obtained a segregation of SnO_2-type nanodomains in the interphasing MgAl-LDH sand-rose region. Using XAS and Möss-bauer spectroscopies, Intissar et al. [12] have, also, proved that the incorporation of tetravalent cations in octahedral sheets does not occur, but actually an amorphous SnO_2 is formed and impregnates the hydrotalcite crystallites. This secondary phase can act as a generator of new catalytic properties and can contribute to the enhancement of material surface areas.

Due to their amazing properties, layered double hydroxides or hydrotalcite-type compounds have received increased interest in numerous fields, such as catalysis [5,13], photocatalysis [14–17], catalysts support [18], adsorbents [19], anion exchangers [20,21], drug delivery systems [22], and bonding materials. Their appli-

* Corresponding author. Tel.: +40 232 201135.
  E-mail address: m1i2m3i4@yahoo.com (E. Dvininov).

Table 1
Sample characteristics.

Sample	SnO$_2$ theoretical content (wt%)	Hydrolysis agent	Calcination type
MgAl-LDH	–	–	723 K in furnance
Sn$_1$–Mg$_3$Al	10	NH$_4$OH	MW
Sn$_2$–Mg$_3$Al	10	NaOH	MW
Sn$_3$–Mg$_3$Al	10	NH$_4$OH	723 K in furnance
Sn$_4$–Mg$_3$Al	10	NaOH	723 K in furnance
Sn$_5$–Mg$_3$Al	35	NH$_4$OH	MW
Sn$_6$–Mg$_3$Al	35	NaOH	MW
Sn$_7$–Mg$_3$Al	35	NH$_4$OH	723 K in furnance
Sn$_8$–Mg$_3$Al	35	NaOH	723 K in furnance

cability as catalysts and adsorbents highlight their importance in environment remediation.

Although their photocatalytic properties are mainly reduced to some Zn containing materials [17,23], we demonstrate, here, the possibility to use the photocatalytic inactive Mg/Al-layered double hydroxide to improve the photocatalytic activity of SnO$_2$, under mild acidic conditions.

It is well known that SnO$_2$ nanoparticles and some of their derivatives [24–29] show photocatalytic activity under UV irradiation and basic pH values, being used for the organic pollutant degradation from synthetic waste waters. The objective of this work is to investigate the possibility to embed the MgAl-LDH particles in SnO$_2$ domains by simple impregnation of the hydrotalcite with tin chloride followed by hydrolysis and calcination. This will ensure a great increase in the surface areas and a good contact between the two phases.

MgAl-LDH particles in contact with SnO$_2$ act as a barrier layer for charge recombination and electron trap sites leading to a better charge separation. Thus, the resulted SnO$_2$/MgAl-LDH nanocomposites provide enhanced photocatalytic activity by improving the contact between pollutant solutions and photocatalysts and by facilitating a good stability of SnO$_2$ domains intimately mixed with hydrotalcite particles.

In order to demonstrate the photocatalytic activity of the as-synthesized composites, we have investigated the decolourization of methylene blue (MB) solutions, under UV irradiation.

2. Experimental

2.1. Materials and equipments

Mg(NO$_3$)$_2$·6H$_2$O and Al(NO$_3$)$_3$·9H$_2$O have been purchased from Aldrich Chemicals and used without further purification. SnCl$_4$·2H$_2$O was purchased from Fischer Chemicals.

Powder X-ray diffraction patterns (PXRD) were obtained with a Bruker D8 Advance X-ray diffractometer, using Cu Kα radiation (graphite monochromator on the diffracted beam, 40 kV and

40 mA) in a Bragg–Brentano geometry, with Soller and fixed slits, and a NaI (Tl) scintillation detector.

Methylene blue concentration and UV–Vis diffuse reflectance spectra (UV–Vis DRS) of samples were recorded, in the range 200–600 nm, on a Schimadzu 2401 UV–Vis spectrophotometer with an integrating diffuse reflective sphere and BaSO$_4$ as reference.

SEM micrographs were obtained with a Carl Zeiss-type scanning electronic microscope (SEM), 1550 HRSEM equipped with NORAN Vantage series 5 EDX analysis equipment.

TEM imaging was carried out using a Philips CM300ST-FEG microscope equipped with a Kevex EDX detector – with ultra-thin window – and Thermo Noran System Six Analyzer. Samples for TEM were prepared by dropping the dispersion of grinded sample in ethanol onto a carbon coated TEM grid.

BET-specific surface area of starting material and resulted composites were calculated from nitrogen adsorption isotherm determined at 77 K using an Quantachrome Nova 2200 surface analyzer after the sample was outgassed under vacuum at 473 K.

2.2. MgAl-LDH synthesis

MgAl starting hydrotalcite, with the cationic Mg^{2+}/Al^{3+} ratio of 3, was prepared by classical coprecipitation method, at constant pH [5]. Briefly, the synthesis was carried out by the slow addition of the metal nitrate mixture (1 M) to a Na$_2$CO$_3$ solution (1 M), under magnetic stirring, the pH being adjusted to 8 using a 2 M NaOH solution. After precipitation, the slurry was kept for 3 h at room temperature followed by ageing at 343 K for 20 h. The resulted solid was separated by filtration, washed several times with de-ionised water and dried at 353 K over night.

2.3. SnO$_2$/MgAl-LDH composite synthesis

In order to obtain the tin loaded materials, denoted as Sn$_x$–MgAl (x = 1–8), the wet impregnation method was used. For this purpose, ethanolic solutions of SnCl$_4$·2H$_2$O, having different concentrations, were contacted with the dehydrated hydrotalcite (473 K/2 h), in order to obtain two Sn^{4+}/LDH weight ratios: 0.6 and 1.22. After impregnation, the mixtures were treated with 2 M NaOH or 45 wt% NH$_4$OH solutions in order to generate the tin oxide xerogel [30]. The as-prepared solid was separated by filtration, dried at 353 K over night and calcined in the oven at 723 K for 5 h or under microwave (MW) for 60 min at 1000 W (Table 1).

2.4. Photocatalytic tests

The photocatalytic experiments have investigated the UV-assisted degradation of methylene blue (MB), in aqueous solution, at 298 K, over both MgAl-hydrotalcite and SnO$_2$/MgAl-hydrotalcite

Table 2
Chemical composition, lattice parameters and structural properties of SnO$_2$/MgAl-LDH composite.

Samples	Elemental analysis[a] (wt%)			Band gap energy (eV)	Mg:Al:Sn atomic ratio[a]	Al/(Al + Mg) at. ratio	FWHM[b] 2θ	t[c] (Å)	Lattice parameters (Å)	
	Mg	Al	Sn						a	c
MgAl-LDH	63.67	36.33	–	–	1:0.51	0.33	0.534	89.7	3.071	23.756
Sn$_1$–MgAl	59.10	29.03	11.86	4.9	1:0.44:0.04	0.30	0.512	95.4	3.071	23.937
Sn$_3$–MgAl	49.91	24.61	25.48	4.7	1:0.44:0.1	0.30	0.529	86.7	3.068	23.926
Sn$_5$–MgAl	31.97	21.40	46.64	4.3	1:0.52:0.23	0.34	0.404	111.8	3.062	23.914
Sn$_7$–MgAl	25.44	29.77	44.57	4.9	1:0.52:0.6	0.34	0.455	91.8	3.058	23.791

[a] Determined by EDX analysis.
[b] Full width at half-maximum (FWHM) of (0 0 3) plane.
[c] Average crystallite size (t) calculated from (0 0 3) and (0 0 6) reflections using the Debye–Scherrer equation.
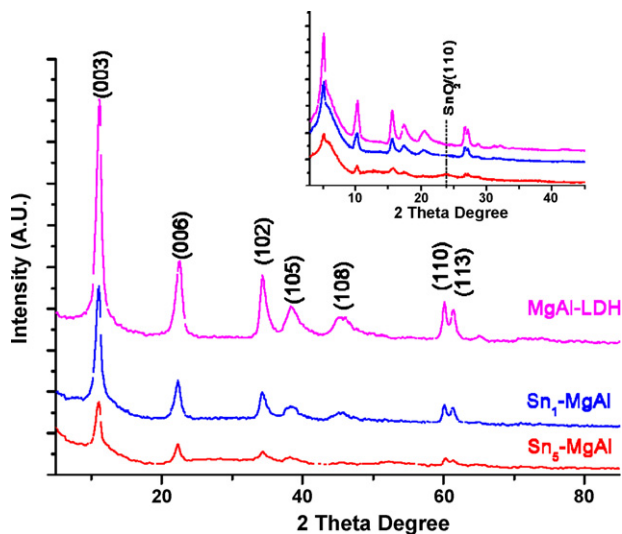
Fig. 1. The influence of Sn content on the XRD patterns obtained using Cu Kα radiation. The inset presents the XRD patterns of the same samples recorded using Mo radiation.

composites using a 6 W Vilber Lourmat UV-lamp with a 254 nm tube. In order to reach the adsorption–desorption equilibrium between the dye and the catalyst surface, the reaction mixtures were stirred for 30 min, in the dark. Moreover, all reactions have been carried out in dark places, in order to avoid the influence of the outer light. In this way the only ones responsible for the dye degradation are being the photons emitted by the UV-source. The solid/liquid ratio (10 mg catalyst/10 ml MB solution) was maintained constant during all measurements, the concentration of MB solution (C_i) being 2×10^{-5} M and a working pH of 5.4. The bleaching of MB solution was investigated by measuring the solution

absorbances during photocatalytic reactions, at 662 nm, using the UV–Vis spectrophotometry.

3. Results and discussions

3.1. Physicochemical properties of SnO$_2$/MgAl-LDH composites

Table 2 summarizes the chemical composition, lattice parameters and band gap energies of a series of synthesized SnO$_2$/MgAl-LDHs composites, while their PXRD patterns are presented in Fig. 1.

The diffraction peaks of the starting hydrotalcite can be indexed in a hexagonal lattice with an R-3m rhombohedral symmetry (Fig. 1). It is known that, for hydrotalcite, the lattice parameter c depends on several factors like anion size, hydratation, and amount of interlayer anion [8]. The lattice parameter a of the LDHs can be correlated with the cation–cation distance within the brucite-like layer. The values of the lattice parameters a and c have been calculated using the following relations [31]: $a = 2d_{110}$, $c = 3d_{003} = 6d_{006}$.

The PXRD patterns of the prepared composites (Fig. 1) show the characteristic features of hydrotalcite-type compounds, the peak intensities decreasing as the tin content increases. After both MW and normal calcinations, no peak characteristic to SnO$_2$ is observed in XRD patterns, recorded using Cu radiation, which indicates that this does not form highly crystalline areas. When Mo radiation, having a shorter wavelength, is used to record the XRD patterns of the composites (inset Fig. 1), coherence domains smaller than the ones observed using Cu radiation can be highlighted. Thus, for the highest tin loaded sample, the appearance of a broad feature, centered at $2\Theta = 23.96°$, which corresponds to the (1 1 0) reflection of SnO$_2$, can be noticed.

Moreover, using the impregnation method to deposit SnO$_2$, a partial substitution of Al^{3+}, in the octahedral layer, with the tin tetravalent cation is impossible. This is sustained by the fact that
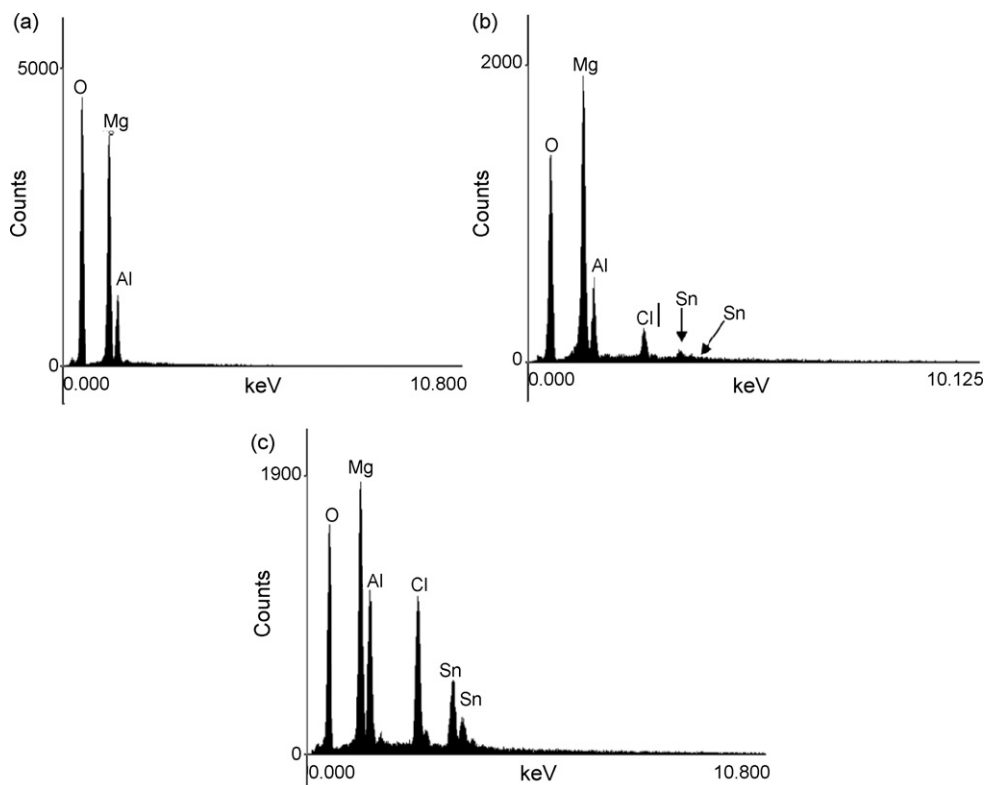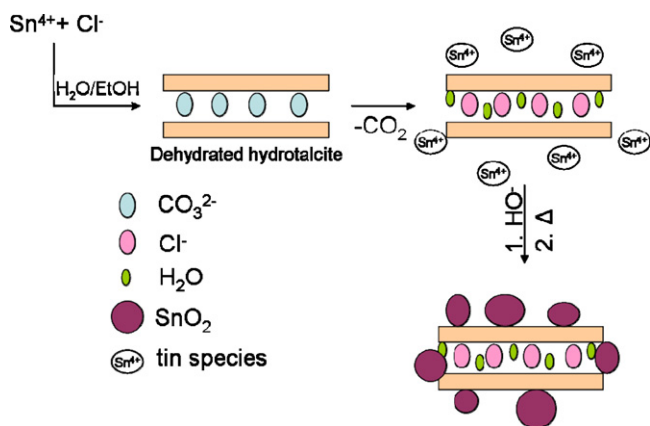

Fig. 2. EDX analysis for (a) MgAl-LDH, (b) Sn$_1$–MgAl, and (c) Sn$_5$–MgAl.

Scheme 1. The draft of the proposed mechanism for hydrotalcite–SnO$_2$ composite formation.
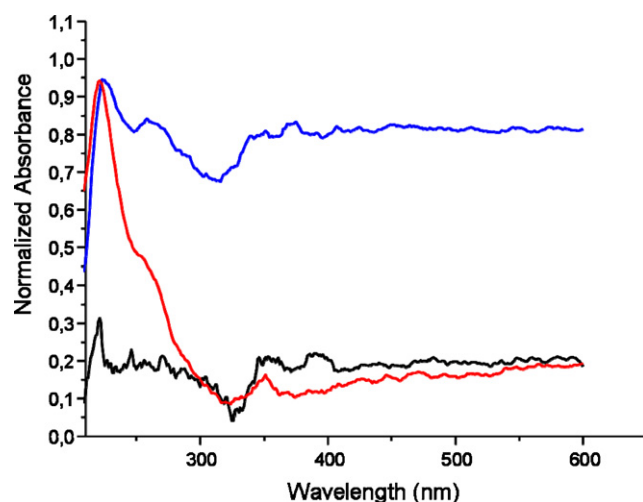

Fig. 3. UV–Vis diffuse reflectance spectra of MgAl-LDH (black), Sn$_1$–MgAl (red) and Sn$_5$–MgAl (blue). (For interpretation of the references to colour in this figure legend, the reader is referred to the web version of the article.)

the lattice parameter a exhibits a slight decrease in its value, after the reaction with tin precursor, and not an increase as would be expected when a smaller trivalent cation, Al^{3+}, having an ionic radius of 0.53 Å, is replaced by a bigger cation-like Sn^{4+} that has a 0.69 Å ionic radius [32].

Due to the heating treatment applied before impregnation, the hydrotalcite loses the interlayer water being able, afterwards, to recover its initial form after rehydration. During the impregnation with SnCl$_4$ ethanolic solution, the hydrotalcite tends to recover its hydrated form by absorbing the water traces present in ethanol. This will be accompanied by a good transport of chloride anions, present in the impregnation solution, to the interlayer space where they replace carbonate anions, as indicated by EDX analyses (Fig. 2). The slight increase of the lattice parameter c (Table 2) during the impregnation process sustains the supposition of the chloride ion intercalation, this having a bigger size than carbonate anion [5]. Moreover, the presence of (001) reflections in the XRD patterns of resulted composites shows that the hydrotalcitic structure is maintained during composite formation and calcination. Using the impregnation method we have obtained a good distribution of tin species, which are represented most probably by α-stannic acid which is soluble in water at room temperature. Under basic conditions, the resulted tin species are negatively charged [33] and can be anchored on hydrotalcite particle surfaces. During the thermal treatment these species will generate SnO$_2$ domains intimately mixed with hydrotalcite particles (Scheme 1).

The LDH phase crystallinity can be estimated through the value of the full width at half-maximum (FWHM) corresponding to either (003) or (006) reflection (Table 2). The decrease of this parameter is opposite to what was observed by other authors for Sn^{4+} incorporation in hydrotalcite octahedral layer [34] and can be correlated with the increase of the phase crystallinity after hydrotalcite particle dispersion within SnO$_2$ domains.

The average crystallite size (Table 2) of the LDH phase has been estimated from the (003) and (006) reflections of the XRD patterns, employing the Debye–Scherrer equation: $t = 0.9\lambda/\beta\cos\theta$, where t is the crystallite size, λ is the wavelength of the used radiation, β is the full width at half-maximum and θ is the Bragg diffraction angle. The size of the LDH's crystallites increases with the increase of Sn content, being higher for the samples calcined in MW and smaller for the normal calcined samples. This thermal behaviour is characteristic of hydrotalcites, as reported that by microwaving a MgAl-LDH the crystallite size increases [35].

The EDX analyses (Fig. 2) show the increase of tin content in the as-prepared samples as a function of its concentration in the starting solution. At the same time, the increase of chloride content in the same direction can be observed. As the Mg/(Mg + Al) atomic

ratio remains relatively constant during impregnation, this increase cannot be attributed to the increase of the electrical charge density of layers (that can be generated by Al^{3+} substitution with Sn^{4+}), but can be explained by the fact that CO$_3{}^{2-}$ ions are replaced by Cl$^-$ ions during the treatment with SnCl$_4$ ethanolic solution. In order to verify this supposition, we have recorded the FTIR spectra of a series of prepared composites (not shown here) and we have observed the decrease of the intensity of the band corresponding to carbonate ion with the increase of chloride content in EDX data.

As it has been reported previously [36,37], tin cations can adopt both octahedral and tetrahedral coordinations, which can be easily distinguished in UV–Vis diffuse reflectance spectra. Based on the literature reports, it can be concluded that the absorption observed at 260 nm can be assigned to hexacoordinated polymeric Sn–O–Sn type species. The intensity of this absorption increases with the tin content of the prepared samples. Moreover, the presence of absorption at about 220 nm can be noticed in the UV–Vis spectra of the samples. This absorption can be associated with the amorphous nature of SnO$_2$ [10], suggesting that tin cations are surrounded by a smaller number of oxygen anions than in octahedral coordination which is similar to SnO$_2$-like xerogel [38]. Once the tin loading increases, the decrease of the ratio between the absorption intensities corresponding to tetrahedral or octahedral coordination can be noticed. These observations are well correlated with XRD data (inset Fig. 1) showing the presence of SnO$_2$ crystalline phase.

In order to obtain details about light absorptive properties of the as-synthesized materials, we have estimated their band gap energies, by representing the α–E dependences and analyzed the sharp absorption region. The α parameter can be represented by the relation: $\alpha E = B(E - E_g)^p$ [39], where B is a constant that depends on the transition probability and p is an index that characterizes the optical absorption process and its theoretical value is equal to 2, 1/2, 3 and 3/2 for indirect, direct, allowed indirect forbidden and direct forbidden transitions, respectively. The best linear plots were obtained for $(\alpha E)^2 - E$ dependences which allowed us to estimate the band gap energies as having values between 4.6 and 5 eV. As MgAl-LDH is optically transparent (Fig. 3), the present absorption features can be attributed to O^{2-}(2p) → Sn^{4+}(4d) transition. This energy is bigger than that of the SnO$_2$ (3.2–3.8 eV) [4,40], and can be explained through the partial amorphous character of the SnO$_2$ component.

SEM images of the prepared composites indicate the maintenance of the plate-like shape of the hydrotalcite particles (Fig. 4a–d) embedded by SnO$_2$ domains. Moreover, it can be remarked that
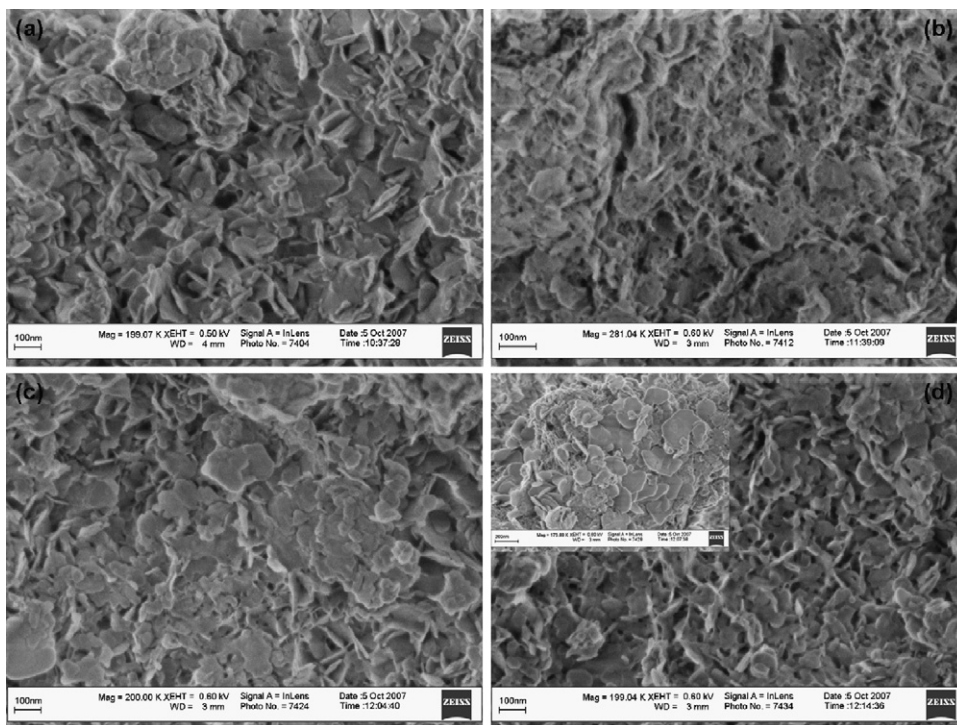
Fig. 4. SEM images of Sn_1–MgAl (a), Sn_2–MgAl (b), Sn_3–MgAl (c) and Sn_4–MgAl composites. The inset in (d) shows a lower magnification SEM image of Sn_4–MgAl sample.

SnO_2 forms a highly porous network intimately mixed with hydrotalcite particles and is responsible for the high surface areas shown by these materials (Table 3).

Related to the thermal behaviour of MgAl-hydrotalcite-type compounds, Kanezaki [41] has observed three temperature regions in high temperature X-ray diffractions: (i) the first one appears below 473 K and corresponds to hydrotalcite dehydration, (ii) the second one (473–653 K) corresponds to hydrotalcite decarbonatation and dehydroxylation, while the last one (iii) starts above 673 K and corresponds to the appearance of MgO and, finally, the spinel phase appears at higher temperatures (1173 K). Moreover, it has been proposed by Chepik et al. [30] that SnO_2 can be crystallized from its xerogel, formed by reacting $SnCl_4 \cdot 2H_2O$ (in buthanol) with ammonia, at 873 K. In order to preserve the memory effect of the hydrotalcite we preferred to perform the samples' calcination at a lower temperature (723 K). The exposed composites to air, after the calcination, did not show the presence of neither MgO nor $MgAl_2O_4$, as detected by XRD measurements. As a result, we can conclude that the presence of SnO_2 will not influence the properties of the hydrotalcite component.

The TEM images indicate the alternation of large and intimately mixed SnO_2/MgAl-LDH areas with small tin-free areas (Fig. 5). Similar results have been obtained by Intissar et al. [10] when

they have tried to incorporate Sn^{4+} in the octahedral layer of Co/Al-hydrotalcite using coprecipitation method, at constant pH. Moreover, it can be observed that hydrotalcite particles, which are not involved in the segregation have a needle-like shape (Fig. 5). These tin-free areas having needle-like particles observed in TEM images are actually small areas arisen from non-homogeneity of the impregnation process which undergo the same thermal behaviour as MgAl-layered double hydroxides.

3.2. Photocatalytic experiments

A photocatalytic process is initiated when a semiconductor absorbs photons having energies higher than its band gap energy. This will lead to the promotion of an electron from valence band to conduction band and will generate holes in valence band. The photogenerated species migrate to the surface where can be implied in reductive (electrons) or oxidative (holes) processes can recombine due to the defects present at this level. The main species involved in the dye molecule degradation are the hydroxyl radicals resulted from both oxidation and reduction of water molecules. The reduction of water molecule takes place through the reduction of oxygen molecules, adsorbed on the catalyst surface, by electrons, the resulted species ($O_2^{-\bullet}$) playing a role in further conversion of water molecule [42] to $HO^\bullet$ radicals.

It is well known that SnO_2, which is an n-type semiconductor, has various applications being used especially for obtaining gas sensors [43,44]. Due to its physicochemical properties, tin oxide may be used as photocatalyst (E_g = 3.2–3.8 eV) [45], under UV irradiation, its efficiency depending on particle size and working pHs. The photocatalytic efficiency of SnO_2 [29,46] for organic molecules mineralization is relatively low, and more attention is paid to its derivatives.

3.2.1. Methylene blue photolysis and absorptive properties of the as-prepared materials

In order to investigate the photocatalytic activities of the reported materials, we need first to line out few observations

Table 3
MB retention and degradation ability and textural properties of some SnO_2/MgAl-LDH composites.

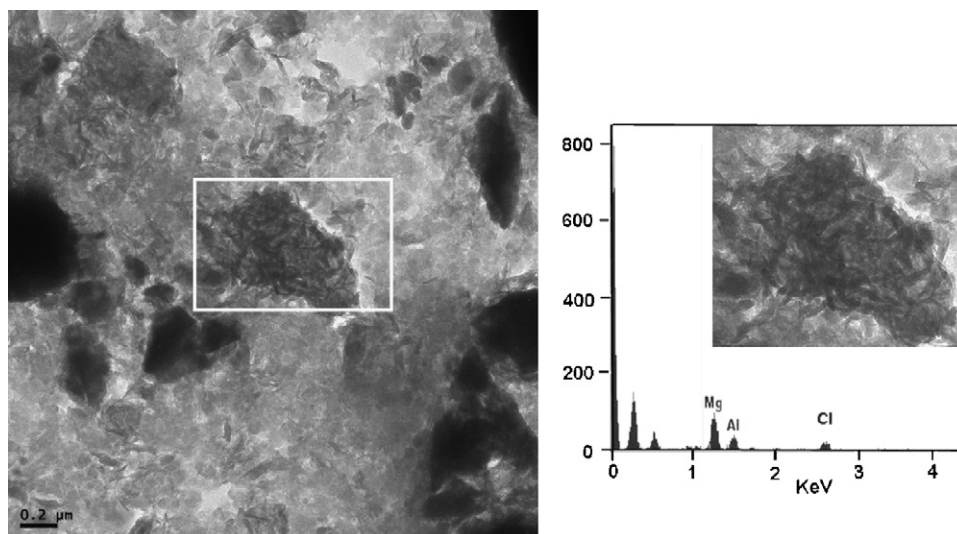| Samples	MW		723 K	
	Sn_2–MgAl	Sn_6–MgAl	Sn_4–MgAl	Sn_8–MgAl
Surface area (m²/g)	408.58	349.92	504.20	266.83
Pore radius (nm)	1.55	1.72	1.53	1.71
Pore volume (cm³/g)	0.805	0.704	0.878	0.526
wt% MB adsorbed	38.73	31.87	25.07	40.41
wt% MB removed after 60 min of irradiation	57.07	97.8	65.81	88.57

Fig. 5. TEM image of Sn_7–MgAl and EDX spectrum of the selected needle-like area.

related to the dye photolysis and absorptive properties of the starting hydrotalcite and prepared composites. It is well known that the dye molecules are very sensitive to the light irradiation. These undergo the photolysis or photobleaching [47] which can be easily mixed up with photocatalysis process when UV–Vis spectroscopy is used to monitor the dye concentration in solution. In order to remove the photolysis suspicions upon used working conditions, we have performed a blank reaction using the same concentration of the dye solution, but without catalysts. We have selected methylene blue (MB) as a model molecule dye which is widely used for photocatalytic investigations. The MB stability against photolysis increases as the pH decreases, but the correction of the pH to lower values than 5.4 (the pH of the as-prepared solution) will lead to the dissolution of hydrotalcite. Thus, we considered convenient to carry on the reaction without a pH correction. Moreover, as SnO_2 alone is photocatalytic inactive under the working pH conditions, the observed photocatalytic activity shall be attributed to the proposed system. Therefore, using a 2×10^{-5} M methylene blue aqueous solution, in the absence of a photocatalyst and without a further pH correction, we have observed that, after 7.5 h under UV irradiation, about 34% of the dye is lost by photolysis (Fig. 6).
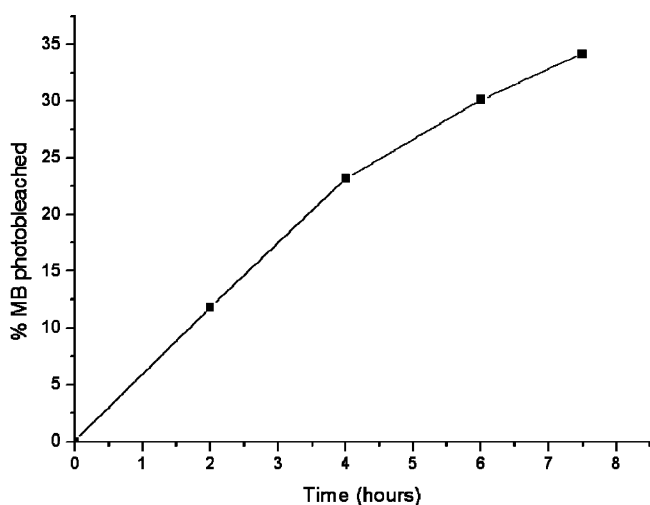
As a catalysis process implies, firstly, the absorption of the species to be degraded at the level of active sites of the catalyst, the capacity of the starting hydrotalcite and the prepared materials to retain methylene blue has to be considered. Fig. 7 shows the absorptive behaviour corresponding to pristine sample and the samples obtained using NaOH as a hydrolysing agent, MW and normally calcined. As it can be observed, Mg/Al-hydrotalcite possesses similar adsorptive capacities for different types of calcination treatment (∼27%). Being a cationic dye, methylene blue cannot be intercalated in the hydrotalcite interlayer space, but it can be adsorbed on the particle surface. The calcined hydrotalcite shows two times higher adsorption capacity for MB than the uncalcined materials for similar cationic dyes [48].

For the prepared composites, we can observe that the absorptive capacity varies due to both tin content and heating treatment. Thus, for the samples that were normally calcined, we can conclude that maximum absorption is obtained for the highest tin loaded material (Sn_8–MgAl, ∼40%), while for the samples calcined under MW the
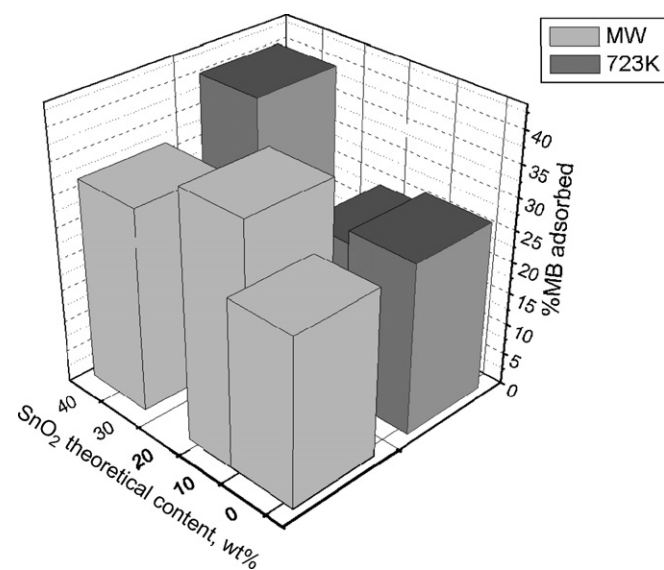

Fig. 6. Methylene blue photolysis under the giving working conditions and in the absence of photocatalyst (pH 5.4, $C_i = 2 \times 10^{-5}$ M).

Fig. 7. The influence of the theoretical SnO_2 content on the efficiency of MB absorption by the samples obtained using NaOH as hydrolysing agent and starting hydrotalcite.
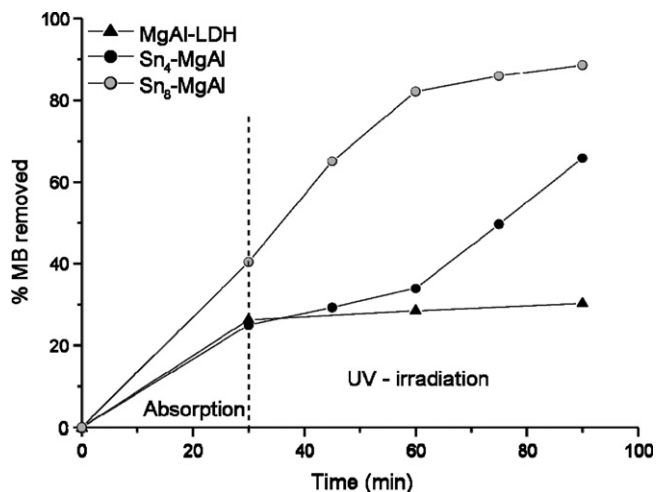
Fig. 8. The efficiency of MB photodegradation as function of theoretical SnO_2 content of the samples obtained using NaOH as hydrolysing agent and calcined at 723 K.

maximum absorption is shown by the lowest tin loaded material (Sn_2–MgAl, ~38%). The MW treatment contributes to the SnO_2-network constriction which will be accompanied by the decrease of the surface area (Table 3), this constriction being more pronounced as the tin content increases. These high absorption capacities can be explained by high surface area shown by these materials, which is generated mainly by SnO_2 domains (Fig. 4 and Table 3). While the starting hydrotalcite shows an 84 m^2/g surface area, for the resulted composites this area presents higher values for the lower tin loaded materials. This can be explained through the increase of the tin oxide phase density as its percentage in the final sample increases. Moreover, when NaOH is used as hydrolysing agent, the samples calcined at 723 K shows a 504 m^2/g surface area while the sample MW calcined shows 408 m^2/g. The increase of the surface area during calcination is well correlated to Intissars' observations [10], the same parameter showing a decrease as the tin loading increases due to the increase of pore size (Table 3). In addition, it is expected that the amount of MB adsorbed onto catalyst to be depend on its surface area. While for the samples calcined under MW this observation is valid, for the samples calcined at 723 K we can observe an inverse process. This suggests the obtainment of different surface textures after normal and MW calcination which allows a different binding of MB molecules.
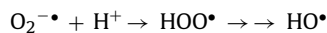
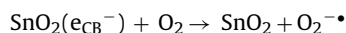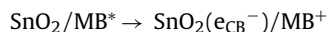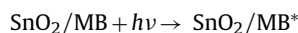### 3.2.2. Effect of tin content and photocatalysis mechanism

In order to have a better view on the photocatalytic mechanism it is important to know the photocatalytic ability of each individual component of the system. The potential for $O_2/O_2^{\cdot}$ reaction to take place is (E) −0.16 eV, versus NHE. As the conduction band of SnO_2, in acidic conditions, has a flat band potential ((E) −0.12 eV versus NHE, pH 5) lower than that needed for $O_2/O_2^{-\bullet}$ reaction, it is obviously clear why this n-type semiconductor is practically inactive for organic compound photodegradation. A further increase of the pH will lead to the shifting of the flat band potential to more negative values which allow the reduction of dissolved oxygen by photogenerated electrons [49].

While SnO_2 is well known as photocatalyst under basic conditions, we have performed further investigations on Mg/Al-hydrotalcite photocatalytic activity and, as it was expected, this does not show any response under UV irradiation (Fig. 8). In this case, the decrease of MB concentration is attributed only to its adsorption on the particle surface. As the photocatalytic activity of
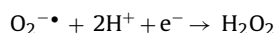
the prepared composites is higher than that of SnO_2 [29,45], used alone for organic compounds degradation, and the hydrotalcite is photocatalytic inactive, it would be interesting to figure out the mechanism of this process.

Bandara and Ranasinghe [49] have reported recently a system based on SnO_2 particles coated by MgO which show a better activity for organic compound degradation than SnO_2. The authors explained this enhanced activity through the negative shifting of the flat band potential which is more pronounced as the pH values and Mg content increase (the flat band potential will shift to more negative values as the Mg content increases from 0 to 20 wt%). Thus, for a 10 wt% MgO loading the flat band potential was found to be −0.9 eV which is more negative than that needed for $O_2/O_2^{-\bullet}$ reaction to take place. This negative shifting of the flat band potential generated by MgO has been understood considering the acidity and the basicity of SnO_2 and MgO, respectively. In SnO_2/MgO systems it is the tendency for deprotonation of SnO_2 surfaces by basic MgO, similar to acid base deprotonation/protonation in solution. In our case, we can attribute the photocatalytic activity of the prepared composites to a similar Mg/Sn coupling. Due to the heating treatment above 673 K [41], magnesium can be partially displaced from octahedral layers and can form with SnO_2 a couple similar to the one described by Bandara and Ranasinghe [49]. Anyway, as the XRD data show, the layered structure of hydrotalcite is recovered in contact with air, so we can assume that the photocatalytic reaction is actually taking place at the interface between SnO_2 and MgAl-LDH particles. As we have not performed measurements of the flat band potentials on our composites, we can assume that the ratio Mg/Sn has a very important influence on photocatalytic activity of the system. While Bandara and Ranasinghe [49] have observed a maximum of activity for a 10 wt% MgO loading, we have observed that the lowest tin loaded materials (high magnesium content) show a weaker activity than higher tin loaded materials (lower magnesium content). Therefore, it seems that we deal with a limitation of Mg-loading till the photocatalytic activity of the system is maximum. As it can be observed in Fig. 8, photocatalytic activity of the samples obtained using NaOH as hydrolysing agent and calcined at 723 K depends on the level of tin loading, the highest loaded material being able to remove ~90% of MB present in solution in 60 min.

As the measured band gap energies of the resulted composites are relatively high, a photosensitized degradation pathway should be considered. Under UV irradiation, methylene blue is able to absorb photons and to transfer the excited electrons into SnO_2 conduction band (Scheme 2). If for SnO_2 itself such a path is energetically unfavourable, due to the negative shifting of the flat band potential, in the SnO_2/MgAl-LDH composites the injected electrons can be further used to reduce oxygen molecules:
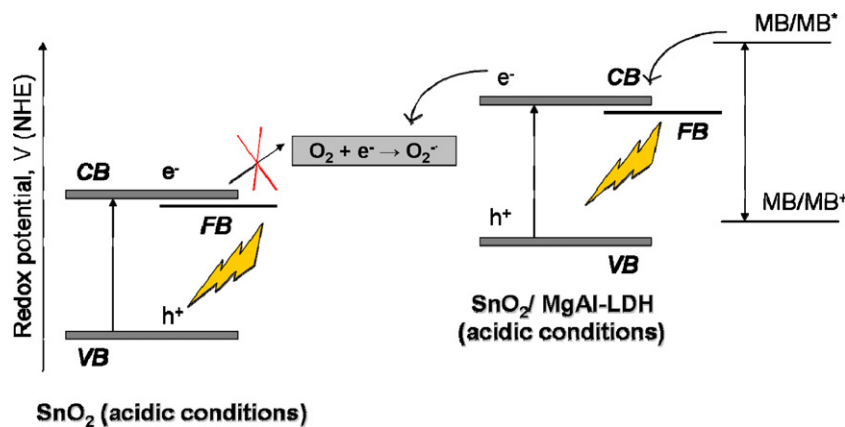
$$SnO_2/MB + h\nu \rightarrow SnO_2/MB^*$$

$$SnO_2/MB^* \rightarrow SnO_2(e_{CB}^-)/MB^+$$

$$SnO_2(e_{CB}^-) + O_2 \rightarrow SnO_2 + O_2^{-\bullet}$$

$$O_2^{-\bullet} + H^+ \rightarrow HOO^\bullet \rightarrow \rightarrow HO^\bullet$$

$$\text{and/or}$$

$$O_2^{-\bullet} + 2H^+ + e^- \rightarrow H_2O_2$$

$$HO^\bullet \text{ or } H_2O_2 + MB \rightarrow \text{degradation}$$

3.2.3. Effect of thermal treatment

If the samples obtained using the same hydrolyzing agent (NaOH) and having a similar tin content are compared (Fig. 9),

Scheme 2. Photocatalytic mechanism of SnO_2 and $SnO_2/MgAl$-LDH composite under acidic conditions.
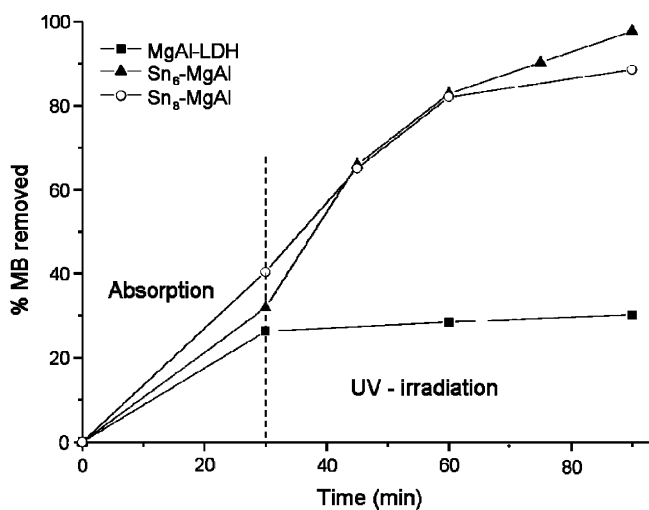

Fig. 9. The influence of calcination method on the MB removal capacity of the prepared composites.

it can be observed that calcination method does not influence significantly the photocatalytic properties of the materials, despite the adsorptive properties which can be slightly different (Table 3).
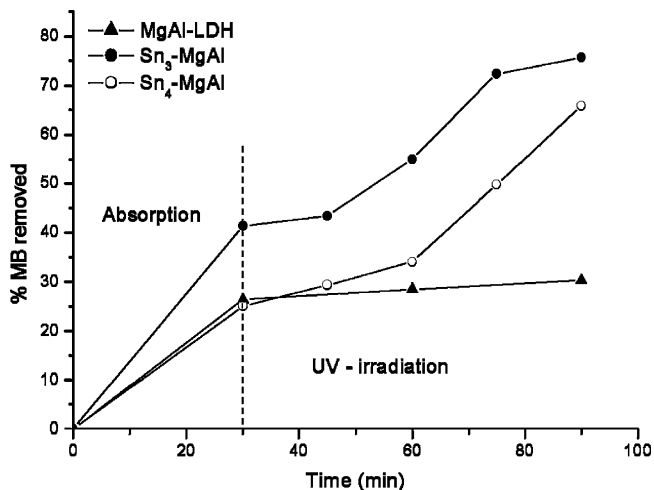

Fig. 10. The influence of hydrolyzing agent on the MB removal capacity of the prepared composites.

3.2.4. Effect of hydrolyzing agent

The effect of hydrolyzing agent on the photocatalytic activity of the samples having a low tin content and calcined at 723 K is shown in Fig. 10. It can be seen that the photocatalytic activity increases for the sample obtained using NaOH for the tin chloride hydrolysis, while their surface area is mainly the same (the surface area of Sn_3–MgAl is ~520 m^2/g). This behaviour resides mainly from the absorption capacity which is better for the sample obtained using NaOH as hydrolyzing agent.

4. Conclusions

In this work we have demonstrated that by impregnation of Mg/Al-LDH with tin chloride, followed by hydrolysis and calcination, the segregation of SnO_2 domains and hydrotalcite particles can be generated similarly to the one obtained by the corresponding cation coprecipitation at constant pH. During this procedure we have preserved the hydrotalcite layered structure, the resulted composites possessing enhanced photocatalytic activity due to $SnO_2/MgAl$-LDH coupling generated through the thermal treatment of the as-prepared composites. This has been proved to be a good way to obtain high surface area materials generated mainly by the presence of SnO_2 porous network. This allows a high absorption capacity of the dye and a good transport of it to the SnO_2/hydrotalcite particle interface. The surface area and absorptive properties of the prepared composites are well correlated in the case of the samples calcined under MW. The samples calcined at 723 K show an atypical behaviour probably due to the modification of surface properties. From the photocatalytic point of view, the calcinations method does not influence significantly the activity of the materials these showing similar degradation properties for similar tin loadings.

While photocatalytic inactivity of Mg/Al-type hydrotalcites is well known, this procedure is able to successfully combine the catalytic and adsorptive properties of layered double hydroxides and semiconducting properties of tin oxide, in order to generate composites which show good activity for methylene blue removed from synthetic waste waters, this activity being a function of both tin content and hydrolyzing agent. While each component of the system, taken separately, is photocatalytic inactive in the given working conditions, we assume that the observed photocatalytic activity of the system is generated by an acid–base interaction of the components which lead to the negative shifting of the flat band potential. This will be energetically favourable for oxygen reduction and consecutive production of hydroxyl radicals responsible for the dye degradation.

Acknowledgements

References

[1] S.V. Awate, K. Suzuki, Enhanced adsorption capacity and photo-catalytic oxidative activity of dyes in aqueous medium by hydrothermally treated titania pillared clay, Adsorption 7 (4) (2001) 319–326.
[2] P. Pichat, H. Khalaf, D. Tabet, M. Houari, M. Saidi, Ti-montmorillonite as photocatalyst to remove 4-chlorophenol in water and methanol in air, Environ. Chem. Lett. 2 (4) (2005) 191–194.
[3] E. Dvininov, E. Popovici, R. Pode, L. Cocheci, P. Barvinschi, V. Nica, Synthesis and characterization of TiO2-pillared Romanian clay and their application for azoic dyes photodegradation, J. Hazard. Mater. 167 (2009) 1050–1056.
[4] C. Wang, X. Wang, B.Q. Xu, J. Zhao, B. Mai, P. Peng, G. Sheng, J. Fu, Enhanced photocatalytic performance of nanosized coupled ZnO/SnO2 photocatalysts for methyl orange degradation, J. Photochem. Photobiol. A: Chem. 168 (2004) 47–52.
[5] F. Cavani, F. Trifiro, A. Vaccari, Hydrotalcite-type anionic clays: preparation, properties and applications, Catal. Today 11 (1991) 173–301.
[6] O. Saber, H. Tagaya, New layered double hydroxide, Zn–Ti LDH: preparation and intercalation reactions, J. Incl. Phenom. Macro. Chem. 45 (2003) 107–115.
[7] O. Saber, B. Hatano, H. Tagaya, Preparation of new layered double hydroxide, Co–Ti LDH, J. Incl. Phenom. Macro. Chem. 51 (2005) 17–25.
[8] S. Velu, K. Suzuki, M. Okazaki, T. Osaki, S. Tomura, F. Ohashi, Synthesis of new Sn-incorporated layered double hydroxides and their thermal evolution to mixed oxides, Chem. Mater. 11 (1999) 2163–2172.
[9] S. Velu, K. Suzuki, M.P. Kapoor, S. Tomura, F. Ohashi, T. Osaki, Effect of Sn incorporation on the thermal transformation and reducibility of M(II)Al-layered double hydroxides [M(II)=Ni or Co], Chem. Mater. 12 (2000) 719–730.
[10] M. Intissar, F. Malherbe, V. Prévot, F.J. Leroux, Evidences of segregated SnO2 type nanoparticles coating layered double hydroxide at moderate temperature, J. Colloid Interf. Sci. 299 (2006) 747–753.
[11] M. Intissar, V. Briois, J.-P. Besse, F. Leroux, Evidence by XAS of tin oxide coating layered double hydroxides, Phys. Scr. T115 (2005) 288–290.
[12] M. Intissar, J.-C. Jumas, J.-P. Besse, F. Leroux, Reinvestigation of the layered double hydroxide containing tetravalent cations: unambiguous response provided by XAS and Mössbauer spectroscopies, Chem. Mater. 15 (2003) 4625–4632.
[13] F. Zhang, X. Xiang, F. Li, X. Duan, Layered double hydroxides as catalytic materials: recent development, Catal. Surv. Asia 12 (2008) 253–265.
[14] S.P.O. Newman, W. Jone, Synthesis, characterization and applications of layered double hydroxides containing organic guests, New J. Chem. 22 (1998) 105–115.
[15] Y. Guo, D. Li, C. Hu, E. Wang, Y. Zhou, S. Feng, Photocatalytic degradation of aqueous organochlorine pesticide on the layered double hydroxide pillared by paratungstate A ion, Mg12Al6(W7O24)·4H2O, Appl. Catal. B: Environ. 30 (2001) 337–349.
[16] A. Patzko, R. Kun, V. Hornok, I. Dekany, T. Engelhardt, N. Schall, ZnAl-layered double hydroxides as photocatalysts for oxidation of phenol in aqueous solution, Colloid Surf. A: Physicochem. Eng. Aspects 265 (2005) 64–72.
[17] E.M. Seftel, E. Popovici, M. Mertens, E.A. Stefaniak, R. Van Grieken, P. Cool, E.F. Vansant, SnIV-containing layered double hydroxides as precursors for nanosized ZnO/SnO2 photocatalysts, Appl. Catal. B: Environ. 84 (2008) 699–705.
[18] L. Barloy, J.P. Lallier, P. Battioni, D. Mansuy, Y. Piffard, M. Tournoux, J.B. Valim, W. Jones, Manganese porphyrins adsorbed or intercalated in different mineral matrices: preparation and comparative, New J. Chem. 16 (1992) 71–80.
[19] P.C. Pavan, E.L. Crepaldi, G.D. Gomes, J.B. Valim, Adsorption of sodium dodecylsulfate on a hydrotalcite-like compound. Effect of temperature, pH and ionic strength, Colloid Surf. A: Physicochem. Eng. Aspects 154 (1999) 399–410.
[20] M. Meyn, K. Beneke, G. Lagaly, Anion-exchange reactions of layered double hydroxides, Inorg. Chem. 29 (1990) 5201–5207.
[21] E.M. Seftel, E. Dvininov, D. Lutic, E. Popovici, C. Ciocoiu, Synthesis of hydrotalcite-type anions clays containing biomolecules, J. Optoelectr. Adv. Mater. 7 (2005) 2869–2874.
[22] J. Choy, S. Kwak, J. Park, Y. Jeong, J. Portier, Intercalative nanohybrids of nucleoside monophosphates and DNA in layered metal hydroxide, J. Am. Chem. Soc. 121 (1999) 1399–1400.
[23] W. Meng, D.G. Evans, X. Duan, Photocatalytic activity of highly porous zinc ferrite prepared from zinc–iron(III)-sulfate layered double hydroxide precursor, J. Porous Mater. 11 (2004) 97–105.
[24] K. Vinodgopal, P.V. Kamat, Enhanced of photocatalysis degradation of an azo dye using SnO2/TiO2 coupled semiconductor thin films, Environ. Sci. Technol. 29 (1995) 841–845.
[25] H.L. Xia, H.S. Zhuang, T. Zhang, D.C. Xiao, Photocatalytic degradation of Acid Blue 62 over CuO–SnO2 nanocomposite photocatalyst under simulated sunlight, J. Environ. Sci. 19 (2007) 1141–1145.
[26] H. Xia, H. Zhuang, T. Zhang, D. Xiao, Visible-light-activated nanocomposite photocatalysts of Fe2O3/SnO2, Mater. Lett. 62 (2008) 1126–1128.
[27] C. Wang, B.-Q. Xu, X. Wang, J. Zhao, Preparation and photocatalytic activity of ZnO/TiO2/SnO2 mixture, J. Solid State Chem. 178 (2005) 3500–3506.
[28] W.W. Wang, Y.J. Zhu, L.-X. Yang, ZnO–SnO2 hollow spheres and hierarchical nanosheets: hydrothermal preparation, formation mechanism and photocatalytic properties, Adv. Funct. Mater. 17 (2007) 59–64.
[29] L. Kórösi, J. Németh, I. Dékány, Structural and photooxidation properties of SnO2/layered silicate nanocomposites, Appl. Clay Sci. 27 (2004) 29–40.
[30] L.F. Chepik, E.P. Troshina, T.S. Mashchenko, D.P. Romanov, A.I. Maksimov, O.F. Lutskaya, Crystallization of SnO2 produced by sol–gel technique from salts of tin in different oxidation states, Russ. J. Appl. Chem. 74 (2001) 1617–1620.
[31] M. del Arco, R. Trujillano, V. Rives, Cobalt–iron hydroxycarbonates and their evolution to mixed oxides with spinel structure, J. Mater. Chem. 8 (1998) 761–767.
[32] R.D. Shannon, Revised effective ionic radii and systematic studies of interatomic distances in halides and chalcogenides, Acta Crystallogr. Sect. A 32 (1976) 751–767.
[33] Y.-I. Lee, K.-J. Lee, D.-H. Lee, Y.-K. Jeong, H.S. Lee, Y.-H. Choa, Preparation and gas sensitivity of SnO2 nanopowder homogenously doped with Pt nanoparticles, Curr. Appl. Phys. 9 (2009) S79–S81.
[34] S. Velu, K. Suzuki, T. Osaki, F. Ohashi, S. Tomura, Synthesis of new Sn incorporated layered double hydroxides and their evolution to mixed oxides, Mater. Res. Bull. 34 (1999) 1707–1717.
[35] S. Möhmel, I. Kurzawski, D. Uecker, D. Müller, W. Gebner, The influence of a hydrothermal treatment using microwave heating on the crystallinity of layered double hydroxides, Crystallogr. Res. Technol. 37 (2002) 359–369.
[36] N.K. Mal, A.V. Ramaswamy, Hydroxylation of phenol over Sn-silicalite-1 molecular sieve: solvent effects, J. Mol. Catal. A: Chem. 105 (1996) 149–158.
[37] K. Chaudhari, T.K. Das, P.R. Rajmohanan, K. Lazar, S. Sivasanker, A.J. Chandwadkar, Synthesis, characterization and catalytic properties of mesoporous tin-containing analogs of MCM-41, J. Catal. 183 (1999) 281–291.
[38] R. Van Grieken, C. Martos, M. Sanchez-Sanchez, D.P. Serrano, J.A. Melero, J. Iglesias, A.G. Cubero, Synthesis of Sn-silicalite from hydrothermal conversion of SiO2–SnO2 xerogels, Micropor. Mesopor. Mater. 119 (2009) 176–185.
[39] J.I. Pankove, Optical Processes in Semiconductors, Prentice-Hall, New Jersey, 1971.
[40] A. Hagfeldt, M. Graetzel, Light-induced redox reactions in nanocrystalline systems, Chem. Rev. 95 (1995) 49–68.
[41] E. Kanezaki, Thermal behavior of the hydrotalcite-like layered structure of Mg and Al-layered double hydroxides with interlayer carbonate by means of in situ powder HTXRD and DTA/TG, Solid State Ionics 106 (1998) 279–284.
[42] J. Zhao, C. Chen, W. Ma, Photocatalytic degradation of organic pollutants under visible light irradiation, Top. Catal. 35 (2005) 269–278.
[43] S.G. Ansari, P. Boroojerdian, S.R. Sainkar, R.N. Karekar, R.C. Aiyer, S.K. Kulkarni, Grain size effects on H2 gas sensitivity of thick film resistor using SnO2 nanoparticles, Thin Solid Films 295 (1997) 271–276.
[44] T.G.G. Maffeis, G.T. Owen, M.W. Penny, T.K.H. Starke, S.A. Clark, H. Ferkel, S.P. Wilks, Nano-crystalline SnO2 gas sensor response to O2 and CH4 at elevated temperature investigated by XPS, Surf. Sci. 520 (2002) 29–34.
[45] Y.R. Park, K.J. Kim, Sputtering growth and optical properties of [1 0 0]-oriented tetragonal SnO2 and its Mn alloy films, J. Appl. Phys. 94 (2003) 6401–6404.
[46] M. Zhang, G. Sheng, J. Fu, T. An, X. Wang, X. Hu, Novel preparation of nanosized ZnO–SnO2 with high photocatalytic activity by homogeneous co-precipitation method, Mater. Lett. 59 (2005) 3641–3644.
[47] A. Mills, J. Wang, Photobleaching of methylene blue sensitized by TiO2: an ambiguous system? J. Photochem. Photobiol. A: Chem. 127 (1999) 123–134.
[48] J. Orthman, H.Y. Zhu, G.Q. Lu, Use of anion clay hydrotalcite to remove coloured organics from aqueous solutions, Sep. Purif. Technol. 31 (2003) 53–59.
[49] J. Bandara, R.A.S.S. Ranasinghe, The effect of MgO coating on photocatalytic activity of SnO2 for the degradation of chlorophenol and textile colorants; the correlation between the photocatalytic activity and the negative shift of flatband potential of SnO2, Appl. Catal. A: Gen. 319 (2007) 58–63.